Hindawi
Journal of Nanomaterials
Volume 2020, Article ID 4515432, 7 pages
https://doi.org/10.1155/2020/4515432

*Research Article*

# Electrical Behavior of Liquid Crystal Devices with Dielectric Nanoparticles

**Vicente Marzal**,[1] **Manuel Caño-García**,[2] **Juan Carlos Torres**,[1] **Xabier Quintana**,[3] **Isabel Pérez**,[1] **and Braulio Garcia-Camara**[1]

[1]*Displays and Photonics Applications Group, Carlos III University of Madrid, 28911 Leganés, Madrid, Spain*
[2]*Department of Nanophotonics, Ultrafast Bio- and Nanophotonics Group, INL-International Iberian Nanotechnology Laboratory, Av. Mestre Jose Veiga s/n, 4715-330 Braga, Portugal*
[3]*CEMDATIC, E.T.S.I. Telecommunication, Polytechnic University of Madrid, Avda. Complutense 30, 28040 Madrid, Spain*

Correspondence should be addressed to Isabel Pérez; isaper@ing.uc3m.es

Received 31 July 2019; Revised 7 January 2020; Accepted 16 January 2020; Published 30 January 2020

Academic Editor: Silvia Licoccia



Nowadays, the development of new devices based on liquid crystal (LC) materials requires improved tuning characteristics according to the application. One approach for this improvement is the use of nanomaterials with the capability of modifying the effective properties of the doped LC mixture. In this work, we analyze the electrical behavior of a titanium dioxide ($TiO_2$) nanoparticle-doped liquid crystal cell using an equivalent circuit. The circuit parameters have been obtained using the impedance spectroscopy technique and time response measurements. The particularity of the samples designed is that the nanoparticles are not dispersed in the LC. Instead of that, nanoparticles are randomly deposited on one of the electrodes. Measurements show that the presence of the nanoparticles increases the temperature sensitivity of the equivalent cell capacitance and the capacitance difference between switched and nonswitched states. These results could be quite useful in the design of novel liquid crystal electronic devices and sensors.

## 1. Introduction

Nematic liquid crystals (NLCs) are present in a large number of current devices, ranging from the well-known liquid crystal displays (LCDs) [1] to different kind of sensors (e.g., biological, temperature, chemical) [2–4] or integrated photonic devices [5, 6]. For this reason, the research on them is still an important topic. Additionally, technological advances demand novel requirements and then novel electrooptical responses of these materials. In this sense, there is a large amount of works focus on the development of new NLCs with tuned characteristics according to the application requirements. While one approach is designing and synthesizing new LC compounds [7], other one is by using nanomaterials with the capability of modifying the effective properties of the doped LC mixture [8].

Depending on the nanoparticle nature, the modification of the LC properties differs. In this sense, we can find the use of metallic [9], dielectric [10], semiconductor [11], or ferroelectric [12] nanoparticles (NPs), among others. This method to vary the electrooptical properties of the LC is considered cost-effective and simple in comparison to the design and synthesis of new LC materials. The final properties of the doped LC mixture strongly depend on parameters such as the NP concentration, their purity, shape, and size, and their refractive index [13, 14]. This leads to a myriad of results in the bibliography. From a general point of view, these NPs behave as impurities affecting to the presence and mobility of ions in the mixture. In this sense, the presence of nanomaterials produces an enhancement of the dielectric anisotropy [15], reduction of the threshold voltage [16], and also other interesting effects like frequency modulation [17] and

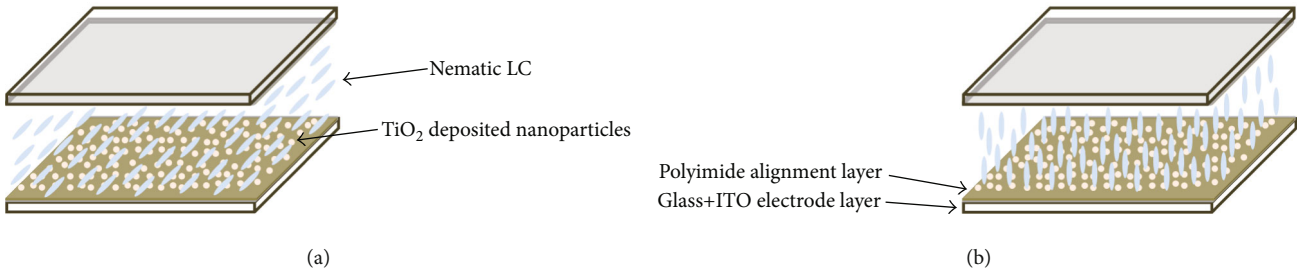


Figure 1: Scheme of the liquid crystal cell with a layer of nanoparticles on one of the substrates. The top substrate includes the ITO and polyimide layer for homogeneous alignment, without nanoparticles. The two different configurations are shown: nonswitched (a) and switched (b) states.

memory effect [18]. Besides these properties, which may be interesting for display applications, other properties could be affected by the presence of the nanomaterials. This is the case of the temperature sensitivity of the electrooptical mixture, which is quite interesting for LC-based temperature sensors [3].

Although there is a large variety of potential materials for the nanoparticles, titanium dioxide ($TiO_2$) nanoparticles are one of the most relevant cases due to their interest in other electrooptical devices [19, 20] as well as in LC mixtures [21–24]. In this work, we analyze the electrical behavior of a $TiO_2$ nanoparticle-doped liquid crystal cell using an equivalent model, as will be explained. In the previous studies, it has been shown that this kind of nanoparticles is able to reduce the screening effect by ion trapping [22]. In contrast, the particularity of the samples of this work is that the nanoparticles are not dispersed in the LC; instead of that, nanoparticles are randomly distributed in one of the electrodes. This cost-effective technique allows a larger control about the distribution and homogeneity of the nanoparticles, as well as a larger lifetime of the cells with the modified properties. We show that the presence of the nanoparticles can get worse the display properties of the liquid crystal while it improves its properties for other kinds of applications. This is the case of the temperature sensitivity of the equivalent capacitance of the cell and the capacitance difference between switched and nonswitched states. We are convinced that these results could be quite useful in the design of the novel liquid crystal electronic devices and sensors in order to accomplish the current specifications of new needs.

## 2. Materials and Methods

*2.1. Sample Fabrication.* In order to obtain the electrical behavior of LC cells with one substrate coated with nanoparticles, we fabricated several ones with the following protocol. The cells were fabricated with two borosilicate Glaston glasses with supertwist polished quality of 0.7 mm uniform thickness and 2.2 cm × 2 cm dimensions. They were coated, in one side, with a 130 nm layer of indium tin oxide (ITO) with a resistivity of 100 Ω/□ and a smoothness of 0.1 $\mu$m/cm, in order to make the electrodes. A polyimide (PI) layer was also used in both glasses for homogeneous alignment of LC. Spacers were used to fix the cell thickness. In particular, silica powder with a diameter of 4.6 $\mu$m was used. Our samples use nanoparticles deposited on one of the substrates of the cell, instead of nanoparticles solved in the LC. For this reason, previously to create the cell, one of the glasses was covered with nanoparticles using a spinner. A graphic outline of a sample cell can be seen in Figure 1.

$TiO_2$ nanoparticles with a diameter of 25 nm (©Avantama) in anatase phase and dispersed in a toluene solution (0.5 wt%) were used. This phase presents a dielectric constant of 18.9 in the considered frequency range [25]. Then, NPs were diluted afterwards in three different concentrations (0.05, 0.005, and 0.0005 wt%) in order to obtain different experimental samples. The considered glass has been covered with the different NPs mixtures using a spin coating and then the samples were kept until the solvent is evaporated and a NPs layer is formed. We check the formation of the layer by both an atomic force microscope (AFM) and an optical microscope in order to observe its uniformity and the formation of clusters, just before and after the formation of the cells and the LC inclusion. The main results are obtained for the concentration of 0.005 wt%, and the results, we show here, correspond to this concentration.

Once the two substrates were ready (one of them with a deposited $TiO_2$ NPs layer), we stuck them with adhesive and a pair of clamps. When the adhesive is cured, we proceed to fill the cell with E7 liquid crystal (©Sigma-Aldrich) by capillarity and to seal it to avoid leaking. In order to normalize later calculations, we use the mean value of the cell area. This value has been calculated as 3.142 $cm^2$ and with a standard deviation of 0.301 $cm^2$.

*2.2. Experimental Setup.* In order to measure the impedance and the electrical capacitance of the experimental LC cells, as well as the temperature dependence of these parameters, two setups were used. The cell was placed in a programmable thermal stage (INSTEC mK2000 model) to keep the temperature constant during each measurement.

The first setup is devoted to measure the impedance of the cells. A Solartron 1260 impedance analyzer, driven by a personal computer, was used to measure both impedance magnitude and phase of the LC-coated cells. Each cell measurement was made at 25°C and 35°C. A measurement frequency range from 10 Hz to 1 MHz and a sinusoidal signal with 30 $mV_{RMS}$ were used. All these electrical variables were processed with the commercial software ZPLOT.

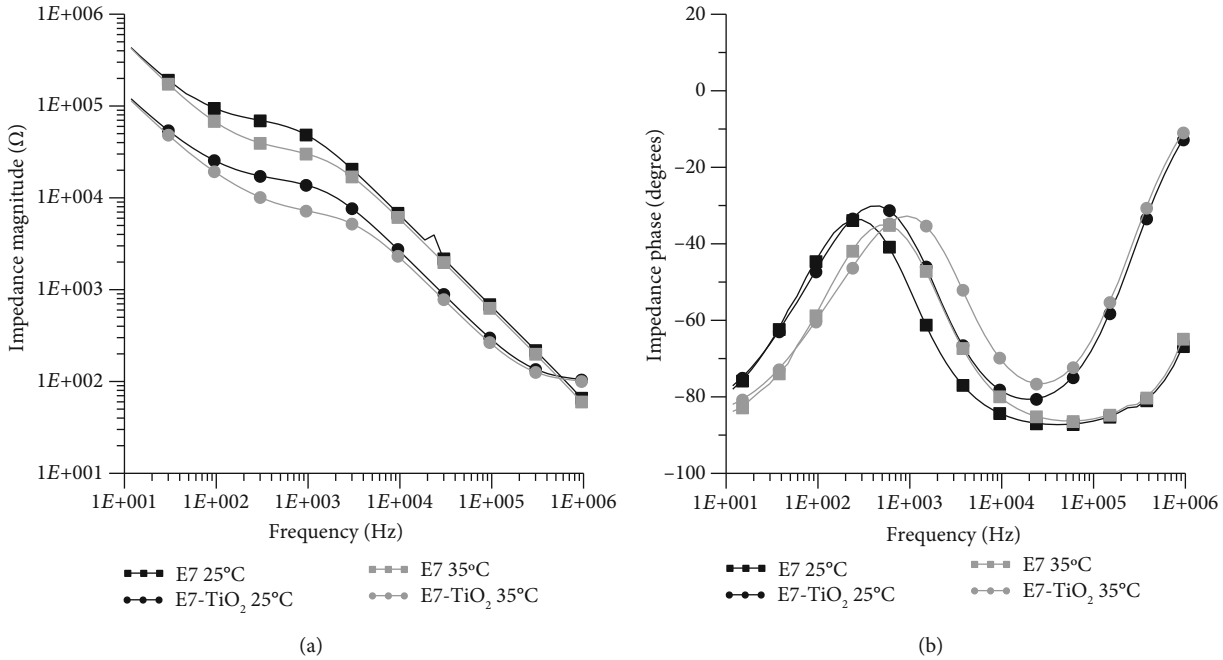


Figure 2: Impedance measurements, magnitude (a) and phase (b), of E7 cells (square symbols) and E7 with a substrate doped with $TiO_2$ nanoparticles, E7-$TiO_2$ (round symbols). Results for temperatures of 25°C (black lines) and 35°C (grey lines) are included.

A second setup has been used for the electrical capacitance measurement. As it is well known, a liquid crystal cell behaves as a parallel-plate capacitor and its electrical capacitance, $C$, has a nonlinear dependence of the applied voltage. By adding an electrical resistance ($R_P$) in series with the LC cell and measuring the rise time ($t_s$) of the system, we can retrieve the value of $C$ by simple calculations ($t_s = 2,2 \cdot R_P \cdot C$) approaching that the device behaves as a first-order system [26].

In order to know the electrical capacitance, we measure the rise time with the oscilloscope while a square signal is applied to the circuit in small voltage steps from an "off" cell state (Figure 1(a)) to the "on" cell state (Figure 1(b)) and we use the previous relationship to deduce the value of $C$.

## 3. Results and Discussion

*3.1. Impedance Measurements.* The impedance (magnitude and phase) of the fabricated planar LC cells, both pure LC (E7) and $TiO_2$-doped E7 (E7-$TiO_2$), was measured using the first setup described in the previous section. These measurements were taken for two ambient temperatures (25°C and 35°C), in order to check the temperature sensitivity of the device, and in a frequency range from 10 Hz to 1 MHz, as explained before. Experimental impedance results are shown in Figure 2. As it was explained, although measurements were made for every considered concentration of the NPs, here we only show those of a 0.005 wt% concentration. This is because it produces the most remarkable results.

The presence of nanoparticles on the substrate can be strongly noticed in the electrical behavior of LC cells, as can be seen in Figure 2. While the magnitude of the impedance, for both temperatures, is lower in the doped case than in a pure LC cell, the maximum of the phase in the medium frequency range is shifted to larger frequencies as we include nanoparticles in the device. This behavior is consequence of the effect of the nanoparticles on the ion mobility as explained in [21, 22]. These impedance graphs also indicate that, from an electrical point of view, the cells can be modeled, in this frequency range, with the equivalent electrical circuit (EEC) shown in Figure 3.

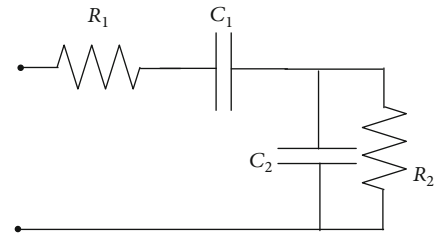


Figure 3: Equivalent electrical circuit of LC cells in the frequency range from 10 Hz to 1 MHz.

Where $R_2$ and $C_2$ model the effect of the LC mixture (parallel-plate capacitor with a nonideal dielectric), $R_1$ is due to the electrodes and $C_1$ takes account of the capacitive effect of the alignment layers at low frequencies. In this study, we want to show how the presence of the nanoparticles may change these parameters.

The E7 cell behaves like an ideal capacitor ($C_2$) in the frequency range from 20 kHz to 200 kHz. In this range and under this dominant capacitance behavior, the magnitude of the impedance is inversely proportional to the frequency while the phase tends to be constant and equal to -90°, as expected. This dominant capacitance is represented in our model as capacitor $C_2$ (Figure 3). The value of $C_2$ can be

Table 1: Values of EEC components of LC cells. The values in columns E7 and E7-$TiO_2$ are the values fitted directly from measurements. The values on columns N-E7-$TiO_2$ are the normalized ones, considering the differences on the active area of experimental samples.

| | Temperature = 25°C | | | Temperature = 35°C | | | Temperature sensitivity | |
|---|---|---|---|---|---|---|---|---|
| | E7 | E7-$TiO_2$ | N-E7-$TiO_2$ | E7 | E7-$TiO_2$ | N-E7-$TiO_2$ | E7 | N-E7-$TiO_2$ |
| $R_1$ (Ω) | 26.5 | 100 | 100 | 26.5 | 100 | 100 | Negligible | Negligible |
| $C_1$ (nF) | 32 | 115 | 88 | 32 | 115 | 88 | Negligible | Negligible |
| $R_2$ (Ω) | 66000 | 16000 | 21000 | 31000 | 7500 | 9800 | -5.3%/°C | -5.3%/°C |
| $C_2$ (nF) | 2.8 | 7 | 5.4 | 3 | 8.5 | 6.5 | +0.7%/°C | +2%/°C |

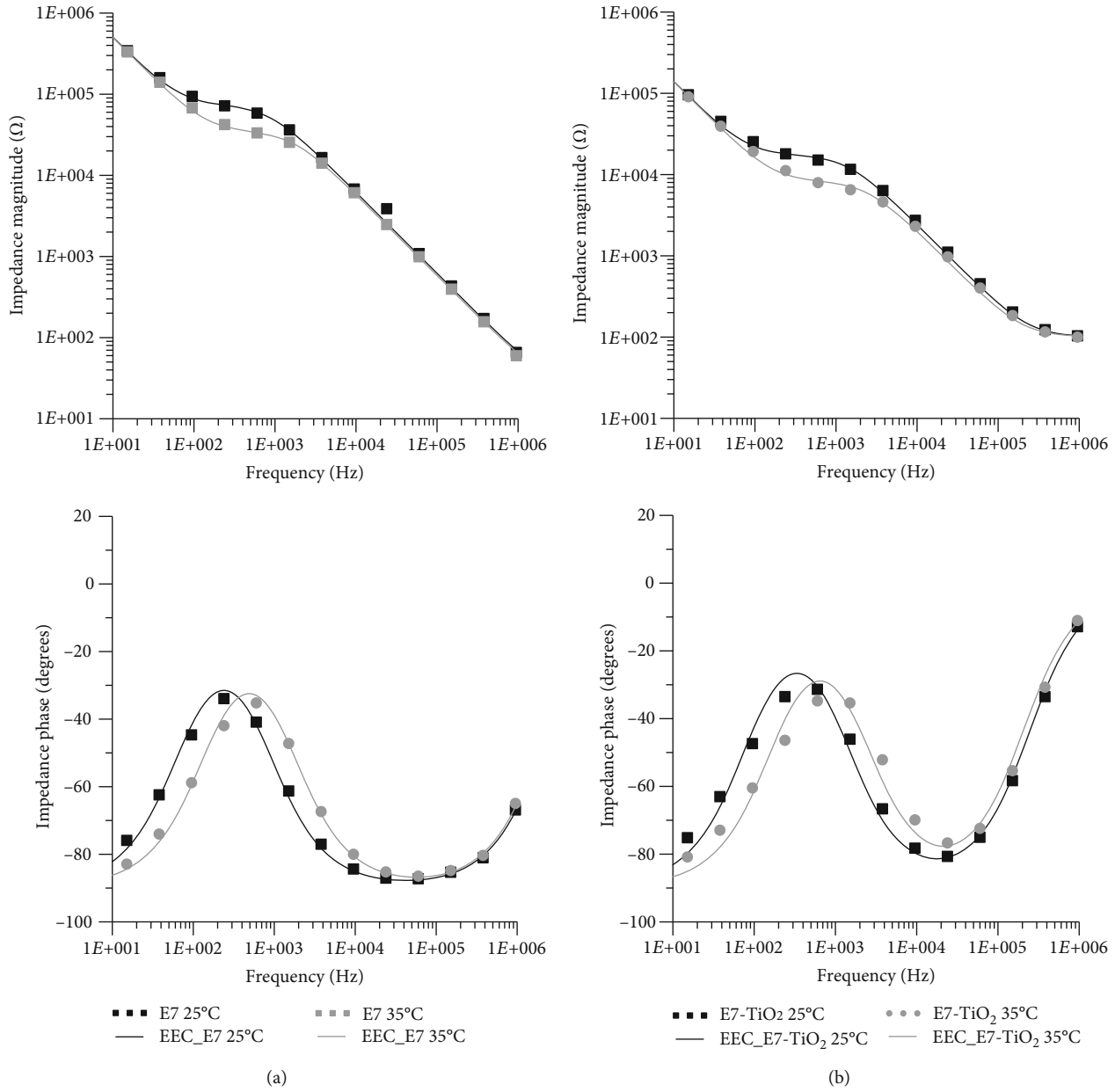


Figure 4: Impedance (magnitude and phase) measurements (symbols) and results from EEC simulation (lines) of E7 cells (a) and E7 with a substrate doped with $TiO_2$ nanoparticles, E7-$TiO_2$ (b). Results for temperatures of 25°C (black) and 35°C (grey) are included.

measured using the second experimental setup with a low amplitude input signal (30 mVp). For the pure LC cell, the obtained results are 2.8 nF at 25°C and 3 nF at 35°C. In a similar way, the electrical behavior of the doped sample, E7-$TiO_2$, also approaches to an ideal capacitor response (lines with circular points in Figure 2), in a narrow frequency range

near of 20 kHz. In this case, the capacitance values of the capacitor $C_2$ of our model are 7 nF at 25°C and 8.5 nF at 35°C.

The values of the remaining EEC components, for the samples under study, are shown in Table 1. Again, differences in the values of $R_1$ of the samples arose. These are due to differences on the electrodes used in the measurements.

For comparison purposes, the capacitance has been normalized considering the differences on the active area of experimental samples. For a plane capacitor with parallel plates, the capacitance $C$ is proportional to the active area, $A$, as $C = K \cdot A$. This capacitance can be written as $C = K \cdot A_N \cdot A'$, where $A_N$ is the value of normalized area and $A'$ is the ratio between the real value of the sample area, $A$, and the normalized value, $A_N$. Hence, $C_N = C/A'$ is the normalized capacitance, that is the equivalent capacitance of a sample with an active area $A_N$.

Figure 4 shows a comparison between the impedance measurements and the results of the simulated equivalent electrical circuit (EEC). In this figure, it can be seen that the accuracy of the proposed model is high, allowing the use of the simplified EEC.

As can be seen in Table 1, the presence of $TiO_2$ nanoparticles in the sample increases the capacitive effects of both $C_1$ and $C_2$ and diminishes the losses resistance $R_2$. On the other hand, the temperature sensitivity of the equivalent capacitance in the kilohertz range ($C_2$) increases with doping. This behavior is quite useful for the design of LC temperature sensors and in particular for those based on its capacitance variation, like those described in [3].

*3.2. Capacitance Measurements.* The other interesting behavior of the considered samples is the voltage dependence of capacitance $C_2$. As it is well known, the capacitance of a planar LC cell increases with the applied voltage. In this part of the work, we analyze the effect of the nanoparticles on this behavior. We also characterized it by using the second experimental setup described in Experimental Setup. Figure 5 summarizes the results obtained for the pure E7 samples and the normalized ones (considering differences on the active area of experimental samples) of the E7-$TiO_2$-doped cells (N-E7-$TiO_2$).

When the electric field is applied across the cells with $TiO_2$ NPs, the free ion carriers transporting between the electrodes get trapped by $TiO_2$ NPs and the free moving ions decrease. Hence, the screening effect decreases, and when an external field is applied, the force over the LC molecules increases and the threshold voltage decreases. Thus, the presence of $TiO_2$ nanoparticles in the sample decreases the voltage where the capacitance starts to change (about 2 $V_{RMS}$ for E7 sample and about 1 $V_{RMS}$ for E7-$TiO_2$ sample) that is related to the threshold voltage of the device. Additionally, the difference of the sample capacitance at the two different states no switched ($C_{2NS}$) and switched ($C_{2S}$) ones ($\Delta C = C_{2S} - C_{2NS}$) also increases with doping. This increment can be useful for the design of systems where a voltage-dependent capacitance is required, like voltage-controlled signal generators [27] with larger tuning ranges. However, as in the previous analysis, the temperature sensitivity of this parameter ($\Delta C$) also increases in doped cells. While from an impedance point of view, this an interesting characteristic for the design of temperature sensors; this temperature variation should be controlled if a high precision in the signal generator frequency is required.

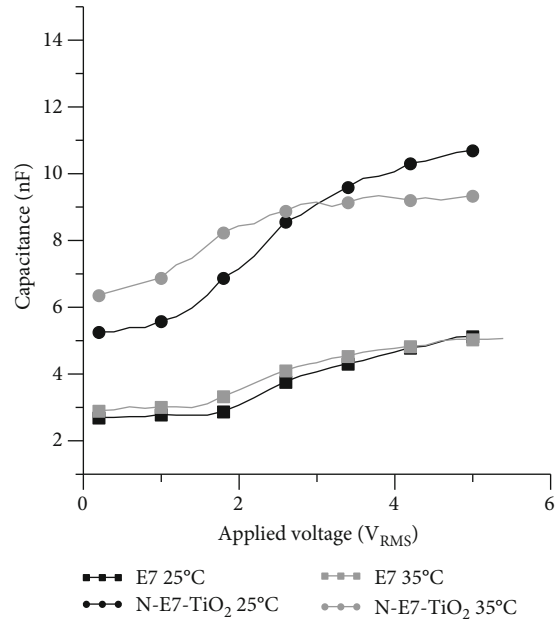


Figure 5: Capacitance of E7 cells (square symbols) and E7 with a substrate doped with $TiO_2$ nanoparticles, normalized considering samples area differences, N-E7-$TiO_2$ (round symbols), as a function of applied voltage. Results for temperatures of 25°C (black lines) and 35°C (grey lines) are included.

A summary of main capacitance values of samples has been included in Table 2.

## 4. Conclusions

In this work, we analyze the electrical behavior of liquid crystal samples doped with $TiO_2$ nanoparticles. Instead of typical doped LC mixtures [15, 16, 21–24], nanoparticles are located on a substrate, forming a layer. Although the presence of nanoparticles is not in the LC volume, we can see that they have interesting effect on the LC cell properties, as expected. In particular, results show that this structure produces an increase of the temperature sensitivity of samples. This kind of behavior is in accordance with other works of LC-NP mixtures in the literature. Then, the presence of nanoparticles in one of the substrates is still strong enough to modify the LC operation. Also, the proposed sample is considered cost-effective and simple in comparison to the use of LC-NP mixtures. The problems of homogeneity and NP precipitation, which are common in doped LC samples, are less important or even negligible in this case.

For the analysis of the electrical behavior of the cells, an equivalent electrical circuit (EEC) has been proposed using the impedance spectroscopy technique and time response measurements. The change of the parameters of this EEC with doping and their temperature sensitivity have been analyzed.

Table 2: Equivalent capacitance of nonswitched cells ($C_{2NS}$), switched cells ($C_{2S}$), and capacitance difference ($\Delta C = C_{2S} - C_{2NS}$) at 25°C and 35°C and temperature sensitivity of these parameters.

| | Temperature = 25°C | | Temperature = 35°C | | Temperature sensitivity | |
|---|---|---|---|---|---|---|
| | E7 | N-E7-TiO2 | E7 | N-E7-TiO2 | E7 | N-E7-TiO2 |
| *C*2NS (nF) | 2.8 | 5.4 | 3 | 6.5 | +0.7%/°C | +2%/°C |
| *C*2S (nF) | 5 | 10.5 | 5 | 9.3 | Negligible | -1.1%/°C |
| $\Delta C$ (nF) | 2.2 | 5.1 | 2 | 2.8 | -0.9%/°C | -4.5%/°C |

The main results of this analysis have been obtained for samples fabricated with a concentration of 0.005 wt%. It can be seen that low concentration is enough to produce observable changes in the LC performance. Large concentrations may produce saturation behaviors, while lower concentrations may be undetectable. Results for this concentration show that the equivalent electrical capacitance of the cells, $C_2$ in Figure 3, is doubled with doping, whereas the loss resistance, $R_2$, is reduced three times. In the case of the dynamic behavior, at 25°C, the increase of the capacitance of doped samples with the applied voltage, $\Delta C$ in Table 2, is twice than in the pure LC ones. Finally, the temperature sensitivity of $C_2$ and $\Delta C$ increases around three times and five times, respectively, when the layer of $TiO_2$ nanoparticles is included in one substrate of the device.

## Data Availability

The data used to support the findings of this study are available from the corresponding author upon request.

## Conflicts of Interest

The authors declare that there is no conflict of interest regarding the publication of this paper.

## Acknowledgments

V.M. wants to express his gratitude to the Ministerio de Economía y Competitividad for his doctoral grant (FPI research fellowship Ref. BES-2014-070410). M.C.-G. wants to express his gratitude to the Ministerio de Economía y Competitividad for his postdoctoral grant (FPI (POP) research fellowship Ref. BES-2014-070964). This research was funded by the Ministerio de Economía y Competitividad, grant numbers TEC2016-77242-C3-1-R and TEC2016-77242-C3-2-R Grant (AEI/FEDER, UE funds) and the Comunidad de Madrid and FEDER program through the SINFOTON2-CM (grant number S2018/NMT-4326) program.

## References

[1] G. Tan, Y. Huang, M.-C. Li, S.-L. Lee, and S.-T. Wu, "High dynamic range liquid crystal displays with a mini-LED backlight," *Optics Express*, vol. 26, no. 13, pp. 16572–16584, 2018.

[2] X. Ding and K.-L. Yang, "Liquid crystal based optical sensor for detection of vaporous butylamine in air," *Sensors and Actuators B: Chemical*, vol. 173, pp. 607–613, 2012.

[3] J. C. Torres, B. García-Cámara, I. Pérez, V. Urruchi, and J. M. Sánchez-Pena, "Wireless temperature sensor based on a nematic liquid crystal cell as variable capacitance," *Sensors*, vol. 18, no. 10, article 3436, 2018.

[4] E. Otón, J. M. Otón, M. Caño-García, J. M. Escolano, X. Quintana, and M. A. Geday, "Rapid detection of pathogens using lyotropic liquid crystals," *Optics Express*, vol. 27, no. 7, pp. 10098–10107, 2019.

[5] F. Peng, Y.-H. Lee, Z. Luo, and S.-T. Wu, "Low voltage blue phase liquid crystal for spatial light modulators," *Optics Letters*, vol. 40, no. 21, pp. 5097–5100, 2015.

[6] J. Kobashi, H. Yoshida, and M. Ozaki, "Planar optics with patterned chiral liquid crystals," *Nature Photonics*, vol. 10, no. 6, pp. 389–392, 2016.

[7] J. F. Algorri, N. Bennis, J. Herman, P. Kula, V. Urruchi, and J. M. Sánchez-Pena, "Low aberration and fast switching microlenses based on a novel liquid crystal mixture," *Optics Express*, vol. 25, no. 13, pp. 14795–14808, 2017.

[8] D. Sikharulidze, "Nanoparticles: an approach to controlling an electro-optical behavior of nematic liquid crystals," *Applied Physics Letters*, vol. 86, no. 3, article 033507, 2005.

[9] Y. Zhang, Q. Liu, H. Mundoor, Y. Yuan, and I. I. Smalyukh, "Metal nanoparticle dispersion, alignment, and assembly in nematic liquid crystals for applications in switchable plasmonic color filters and E-polarizers," *ACS Nano*, vol. 9, no. 3, pp. 3097–3108, 2015.

[10] G. Yadav, M. Kumar, A. Srivastava, and R. Manohar, "$SiO_2$ nanoparticles doped nematic liquid crystal system: an experimental investigation on optical and dielectric properties," *Chinese Journal of Physics*, vol. 57, pp. 82–89, 2019.

[11] D. Zhulai, A. Koval'chuk, S. Bugaychuk, G. Klimusheva, T. Mirnaya, and S. Vitusevich, "Photoconductivity of ionic thermotropic liquid crystal with semiconductor nanoparticles," *Journal of Molecular Liquids*, vol. 267, pp. 406–410, 2018.

[12] Y. Garbovskiy and A. Glushchenko, "Ferroelectric nanoparticles in liquid crystals: recent progress and current challenges," *Nanomaterials*, vol. 7, no. 11, p. 361, 2017.

[13] C.-Y. Huang, C.-C. Lai, Y.-H. Tseng, Y.-T. Yang, C.-J. Tien, and K.-Y. Lo, "Silica-nanoparticle-doped nematic display with multistable and dynamic modes," *Applied Physics Letters*, vol. 92, no. 22, article 221908, 2008.

[14] C.-Y. Huang, J.-H. Chen, C.-T. Hsieh et al., "Effect of the polyimide concentration on the memory stability of the silica-nanoparticle-doped hybrid aligned nematic cell," *Japanese Journal of Applied Physics*, vol. 50, no. 2, article 021702, 2011.

[15] C.-W. Oh, E.-G. Park, and H.-G. Park, "Enhanced electro-optical properties in titanium silicon oxide nanoparticle doped nematic liquid crystal system," *Surface and Coatings Technology*, vol. 360, pp. 50–55, 2019.

[16] M. Urbanski and J. P. F. Lagerwall, "Nanoparticles dispersed in liquid crystals: impact on conductivity, low-frequency relaxation and electro-optical performance," *Journal of Materials Chemistry C*, vol. 4, no. 16, pp. 3485–3491, 2016.

[17] H. Shim, H. K. Lyu, B. Allabergenov, Y. Garbovskiy, A. Glushchenko, and B. Choi, "Enhancement of frequency modulation response time for polymer-dispersed liquid crystal," *Liquid Crystals*, vol. 43, no. 10, pp. 1390–1396, 2016.

[18] M. Middha, R. Kumar, and K. K. Raina, "Photoluminescence tuning and electro-optical memory in chiral nematic liquid crystals doped with silver nanoparticles," *Liquid Crystals*, vol. 43, no. 7, pp. 1002–1008, 2016.

[19] M. M. Khan, S. A. Ansari, D. Pradhan et al., "Band gap engineered $TiO_2$ nanoparticles for visible light induced photoelectrochemical and photocatalytic studies," *Journal of Materials Chemistry A*, vol. 2, no. 3, pp. 637–644, 2014.

[20] J. Fan, Z. Li, W. Zhou et al., "Dye-sensitized solar cells based on $TiO_2$ nanoparticles/nanobelts double-layered film with improved photovoltaic performance," *Applied Surface Science*, vol. 319, pp. 75–82, 2014.

[21] T.-R. Chou, J. Hsieh, W. T. Chen, and C. Y. Chao, "Influence of particle size on the ion effect of $TiO_2$ nanoparticle doped nematic liquid crystal cell," *Japanese Journal of Applied Physics*, vol. 53, no. 7, article 071701, 2014.

[22] P. Kumar, A. Kishore, and A. Sinha, "Effect of different concentrations of dopant titanium dioxide nanoparticles on electro-optic and dielectric properties of ferroelectric liquid crystal mixture," *Advanced Materials Letters*, vol. 7, no. 2, pp. 104–110, 2016.

[23] V. Marzal, J. C. Torres, B. Garcia-Camara, I. Pérez, J. M. Sánchez-Pena, and W. Piecek, "Study of electrical behavior of liquid crystal devices doped with titanium dioxide nanoparticles," *Photonics Letters of Poland*, vol. 9, pp. 22–24, 2017.

[24] R. Katiyar, G. Pathak, A. Srivastava, J. Herman, and R. Manohar, "Analysis of electro-optical and dielectric parameters of $TiO_2$ nanoparticles dispersed nematic liquid crystal," *Soft Materials*, vol. 16, no. 2, pp. 126–133, 2018.

[25] A. Wypych, I. Bobowska, M. Tracz et al., "Dielectric properties and characterisation of titanium dioxide obtained by different chemistry methods," *Journal of Nanomaterials*, vol. 2014, Article ID 124814, 9 pages, 2014.

[26] A. S. Sedra and K. C. Smith, *Microelectronic Circuits*, Oxford University Press, New York, 1998.

[27] C. Marcos, J. M. Sánchez-Pena, J. C. Torres, I. Pérez, and V. Urruchi, "Note: phase-locked loop with a voltage controlled oscillator based on a liquid crystal cell as variable capacitance," *The Review of Scientific Instruments*, vol. 82, no. 12, pp. 126101–126103, 2011.